Regenerative Braking on Bicycles to Power LED Safety Flashers

by

Ian M. Collier

Submitted to the Department of Mechanical Engineering in Partial Fulfillment of the Requirements for the Degree of

Bachelor of Science

at the

Massachusetts Institute of Technology

June 2005

Signature of Author.....
Department of Mechanical Engineering
May 6, 2005

Certified by.....
David Wallace
Associate Professor of Mechanical Engineering
Thesis Supervisor

Accepted by.....
Ernest G. Cravalho
Chairman, Undergraduate Thesis Committee

Regenerative Braking on Bicycles to Power LED Safety Flashers

by

Ian M. Collier

Submitted to the Department of Mechanical Engineering
on May 6, 2005 in Partial Fulfillment of the
Requirements for the Degree of Bachelor of Science in
Mechanical Engineering

Abstract

This work develops a method for capturing some of the kinetic energy ordinarily lost during braking on bicycles to power LED safety flashers. The system is designed to eliminate: (a) battery changing in popular LED flashers, and (b) the "generator drag" associated with battery-less human-powered bicycle lights and flashers. System sizing, mechanical design considerations, potential end-user factors, and a model for braking frequencies in urban settings are discussed. With the urban commuter cyclist in mind as a potential user of the regenerative braking system, custom direct-pull brake calipers (or "V-Brakes") were designed and manufactured to include both conventional friction pads in addition to a DC motor to be used as a generator for kinetic energy capture.

The energy captured by the DC motor during braking is passed through a full wave bridge to a bank of Nickel-Cadmium batteries at an efficiency of 79%. The output of the full wave bridge and the batteries are connected in parallel with a step-down switching voltage regulator, which insulates the LED safety flasher from voltage spikes due to braking at high cycling speeds.

The performance of the final prototype was evaluated at cycling speeds ranging from 8 to 19 mph and braking frequencies ranging from 2 to 8 operations/stops per mile of travel. From the mean power flow (charging) into the batteries per unit distance of travel and the power required by LED safety flashers, the effectiveness of the system at each speed and stopping frequency is examined. For cyclists traveling at average speeds of 10 mph or higher, the LED safety flashers can be powered *continuously* for stopping frequencies of 8 times per mile and *semi-continuously* (> 50% of the time) for stopping frequencies of at least 4 times per mile. As such, the system is determined to be potentially useful to urban commuter cyclists, who frequently perform braking operations at regularly spaced intersections and traffic signals, and who regularly travel by bicycle in low-light conditions (dawn or dusk), though usually less than 50% of the time.

Thesis Supervisor: David Wallace
Title: Associate Professor of Mechanical Engineering

Table of Contents

Table of Figures

1. Introduction

Slowing or stopping operations on bicycles are dissipative. Friction pads applied to the rotating rim of the tire convert kinetic energy of the cyclist and bicycle into heat, which is irrecoverably lost to the atmosphere by conduction and forced convection. This energy could instead be converted into electrical energy and stored for future use. Figure 1.1 illustrates a regenerative braking system that captures energy for storage in a battery and for use by a rear safety flasher.

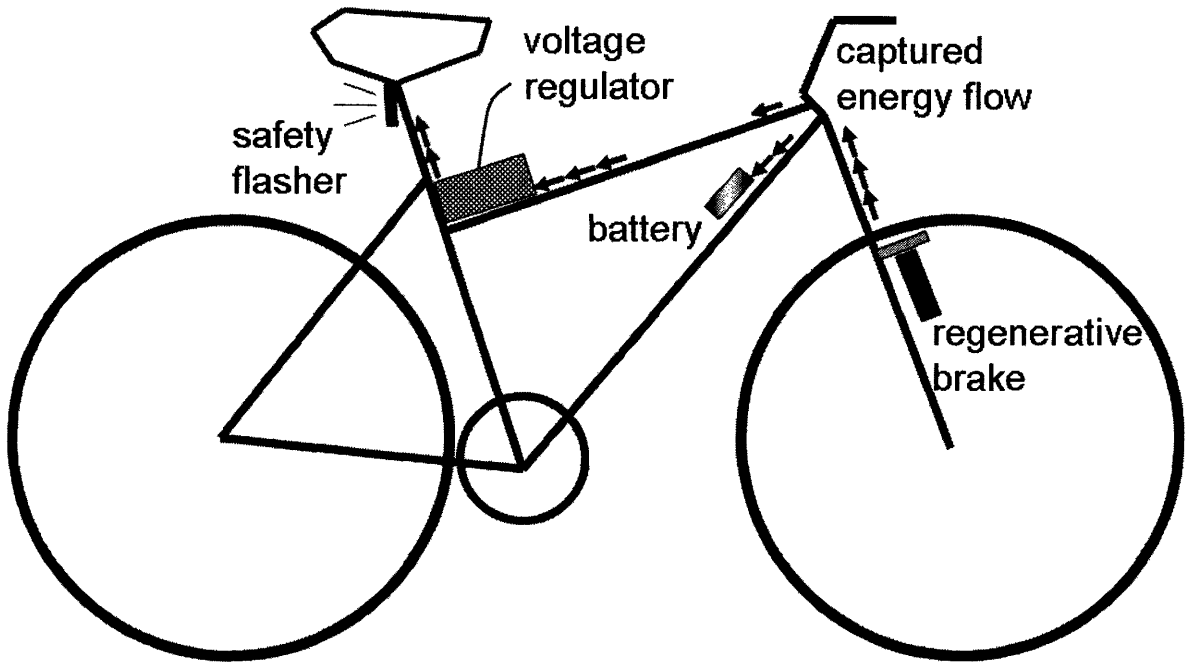

Figure 1.1: A schematic of a bicycle with a system for capturing lost kinetic energy during braking to power a rear safety flasher.

Since this system for powering LED safety flashers uses only energy that would otherwise be lost, the cyclist receives additional functionality from his or her bicycle at no additional cost or physical power output.

Other systems. Though not widely used, hub-integrated and tire contact generators that power bicycle headlamps and rear flashers are currently available for consumer purchase. Both types require additional physical exertion from the cyclist, as they must be engaged continuously to power bicycle headlamps and flashers. Juden reports the results for a series of tests performed by Schmidt, showing that at typical cycling speeds of 20 km/h, 6-14% of the cyclist's physical power output (6-14 W) is used to power headlamps and flashers [1]. Furthermore, even when disengaged, the flow of eddy currents in the armatures of hub-integrated generators dissipates 1-6 W. Juden suggests that this additional "generator drag" is a key drawback, which deters many potential users. Thus, a system capable of similar functionality without requiring additional exertion from the cyclist might be an interesting alternative.

Need for bicycle flashers. The urban bicycle commuter is susceptible to accidents and injury due to the frequent necessity of riding with automobile traffic in low-visibility conditions. Bicycle-automobile accidents occur most frequently at intersections and drives, and account for the vast majority of fatal bicycle accidents. A disproportionate number of such accidents occur during low-light conditions, when fewer cyclists are on the road. A study completed by the Johns Hopkins Injury Prevention Center reports that the death rate per million bicycle trips is 8 times greater between 10 PM and 1 AM than during the hours between 9 AM and 1 PM [2]. To increase night visibility and avoid collisions, most experts recommend the use of (flashing) lights at the rear and front of the bicycle. However, according to a study reported on the Massachusetts Bicycle Coalition's website by Osberg, Stiles, and Asare, only 15% of cyclists in Boston "were observed using *either* a headlight or taillight at night" [3].

In North America, highly efficient battery powered LED lighting systems such as those sold by Cat Eye [4] are popular among commuters and are packaged to meet various power/light intensity needs. Most common among this type are low-power models that conserve energy by flashing. High-power LEDs such as those offered by Luxeon [5] have recently become available for use as bright headlamps on bicycles. All such models are very compact and simple to operate. The only obvious drawback to these types is that they require an occasional change of batteries.

This work develops a consumer product concept for kinetic energy storage during braking operations to power popular LED safety flashers on bicycles. A system for energy recovery (DC motor/generator) and storage (battery) is developed and implemented in the form of a functional prototype, which requires no change of batteries. The actual efficiency and utility of the product are subsequently tested and compared with performance predictions. Finally, future generations and directions for the concept are presented and discussed.

2. System Design

2.1. The physics of braking

Bicycles are generally decelerated by the action of forcing a brake pad against the rim of the front and/or rear wheel. Brake pads are typically made of a rubber-like material, which is chosen for its high friction coefficient when incident with both dry and wet aluminum. A system of lever arms at the brake handle and the brake caliper provide a mechanism for greatly amplifying the braking force at the pad. Consider the direct-pull brakes of typical mountain bikes shown below in Fig. 2.1.1.

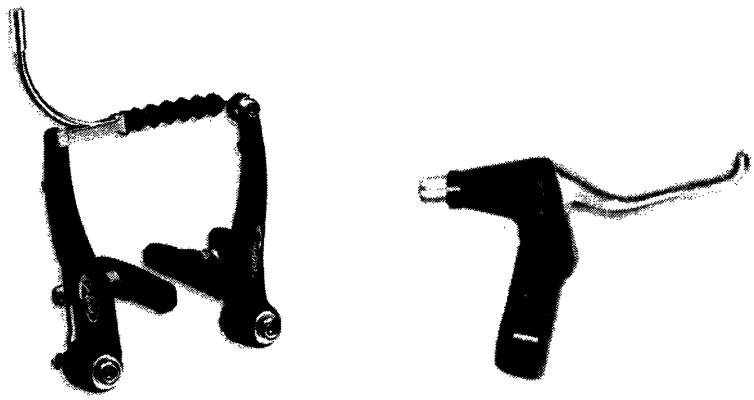

Figure 2.1.1: Typical mountain bicycle direct-pull or "V-Brake" calipers and brake handle.

The force applied by the fingers is amplified by lever arms at both the handle and the calipers to get the force of braking. This mechanical advantage allows the cyclist to easily apply forces sufficient at the brake pad-rim interface to lock the wheels. Additionally, bicycle tires are made of rubber, which has a very high coefficient of friction on cement and asphalt. The result is that decelerations due to braking are usually limited by the location of the center of mass, not by wheel locking.

On bicycles, the center of mass of the bicycle and rider is located far above the wheel contact at the ground and between the two points of wheel contact with the ground. As a result, braking operations using either the front or rear wheel are limited by the reduction of the reaction force at the rear wheel when the mass rapidly decelerates. During rear wheel braking, this results in skidding. In front wheel braking, the rear wheel can lift off of the ground entirely and the rider can be thrown over the handlebars! This is due in part to the high coefficient of friction at the tire-road interface mentioned above.

To understand the limits of possible decelerations on bicycles, consider the maximum deceleration when the reaction force at the rear wheel contact goes to zero. Fig. 2.1.2 below shows both reaction forces, R_{front} and R_{rear}, for the wheel contacts as well as the approximate location of the center of mass (60% rear and 40% front for crouched cyclists) [6].

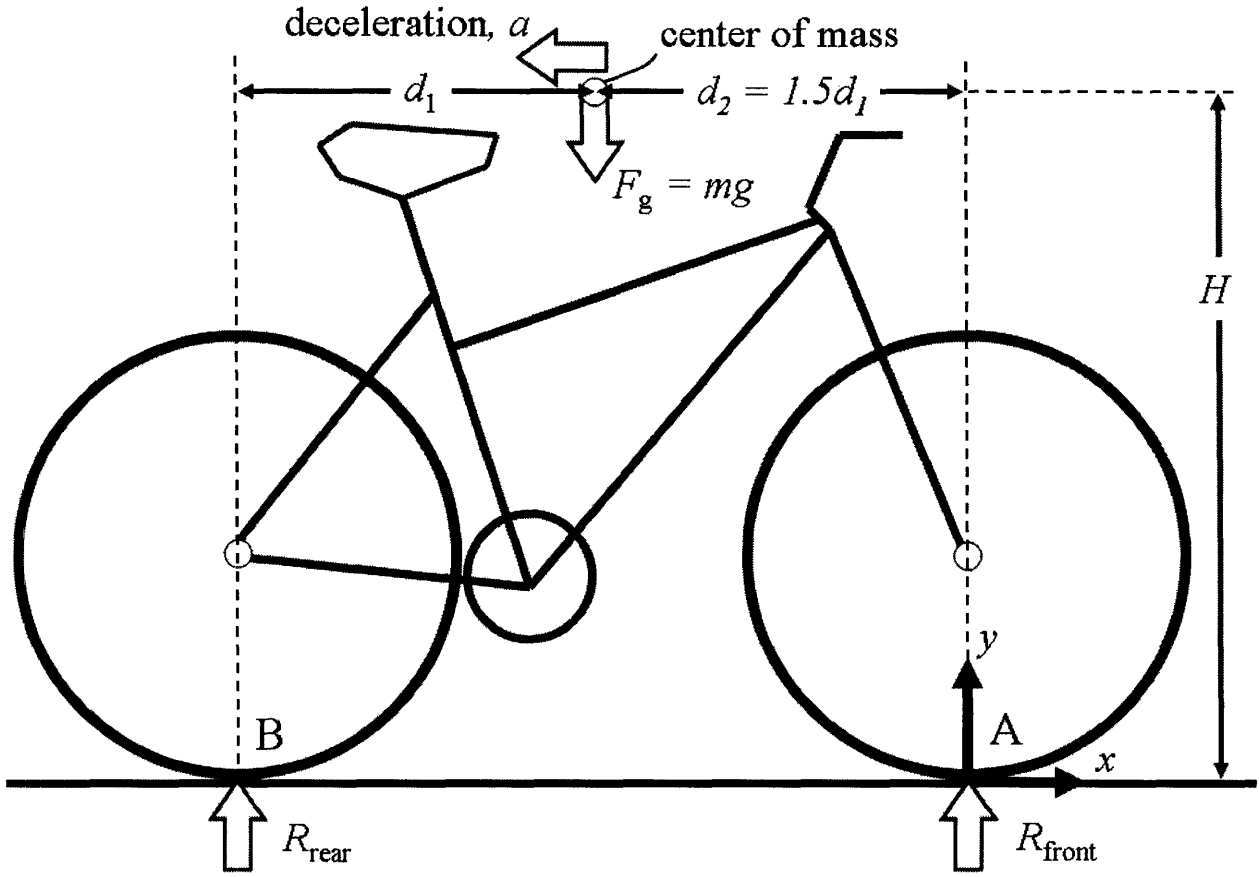

Figure 2.1.2: Diagram of bicycle showing the reaction forces at the front and rear wheels due to the weight and deceleration of the bicycle and rider.

As in Fig. 2.1.2 above for the deceleration, a, balancing the torques about A gives:

$$maH + R_{rear}(d_1 + d_2) = mgd_2 \tag{2.1.1}$$

Since for maximum deceleration, a_{max}, $R_{rear} = 0$:

$$ma_{max}H = mgd_2 \tag{2.1.2}$$

$$\therefore a_{max} = \frac{d_2}{H}g \tag{2.1.3}$$

For typical values of $H = 45$ in. and $d_2 = 25$ in., this results in a maximum deceleration of roughly $0.56g = 5.45$ m/s^2. For comparison, the maximum deceleration possible using only rear braking is less than half at roughly $0.25g$.

This calculation affects the positioning of a regenerative braking system. Since both decelerations require very large energy dissipation at typical cycling speeds, friction pads are

needed at both front and rear brakes. As such, a system for capturing kinetic energy could be placed at the front or rear wheel at the discretion of the rider. However, since the front brake calipers have a higher braking capacity, it is assumed that most riders would choose to place them at the front wheel fork of the bicycle. Fig. 2.1.3 below shows a possible method for coupling a regenerative brake (motor/generator) with a conventional friction pad brake.

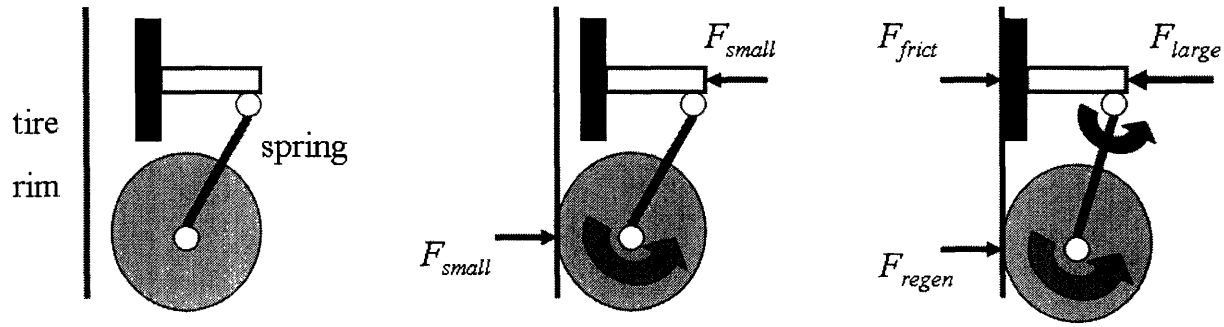

Figure 2.1.3: Diagram showing a two-stage regenerative brake. From left to right: First, when the rider is not using the brakes, both the friction pad and motor wheel are disengaged. Second, as the rider applies light pressure to the brake handle, the motor wheel comes into contact with the rim and begins to rotate. Third, as the rider applies more pressure to the brake handle, the motor wheel is displaced and the friction pad contacts the rim.

2.2. Analysis of available energy

The design of any system involving energy transfer requires an analysis to ensure that the power supply meets the minimum consumption needs of the system. For the case of regenerative braking on bicycles, the critical first step is to determine how commuter cyclists use the braking operation during a typical trip. Incentives to brake (e.g. a red light at a traffic signal) are considered in this section by a model, which incorporates urban traffic signal spacing and timing. As determined from the model, the frequency of braking operations during a trip is used to find an estimate for the mean available power.

2.2.1. Characterization of braking operations for bicycle commuters

There are many instances in cities when it is necessary to use brakes. Near automobile traffic or pedestrians, cyclists commonly brake and decelerate when passing, being passed, moving through narrow spaces, and when stopping entirely. Minimally, however, the urban commuter cyclists considered in this work must brake on approach to traffic signals and turns at intersections – even if no other obstacles exist. As such, it may be appropriate to use traffic signal spacing and timing in cities as a basis for a model to characterize braking operations for urban commuter cyclists.

Though emergency situations necessitating immediate and rapid stops do occur, light braking operations and gradual decelerations are more common [7]. As will become clear in this section, the cyclist benefits from light braking or "feathering" in anticipation of a possible stop. In the case of a red traffic light, the cyclist benefits by feathering his brakes on approach such that if the

light turns green, he may proceed through the intersection with a minimal loss of speed and kinetic energy.

2.2.2. Average continuous power available during a city ride

This section proposes a method for estimating the mean power available to supply LED safety flashers by assuming that a known fraction of the total kinetic energy of the bicycle and rider can be captured and stored by regenerative braking. The model considers typical cycling speeds, urban traffic signal spacing, and an equal probability of arriving at all times during the signal cycle.

The energy available for capture and storage is simply the energy associated with a moving mass – in this case, a bicycle and rider. Recall that the instantaneous kinetic energy, KE, of a bicycle and rider of combined mass, m, at velocity, v, is shown in Eq. 2.2.1:

$$KE = \frac{mv^2}{2}. \tag{2.2.1}$$

If the cyclist were to use his or her brakes and come to a complete stop, this would be the total energy dissipated in that operation. More generally, the energy lost (or captured) in braking is due to a change from initial velocity, v_i, to a final (lower) velocity, v_f. From Eq. 2.2.1, the resulting change in energy, ΔKE, is:

$$\Delta KE = \frac{m}{2}\left(v_f^2 - v_i^2\right). \tag{2.2.2}$$

For a better understanding of how this applies to cycling, it is helpful to think of v_i as typical cruising velocity before braking and of v_f as a fraction of the cruising velocity. Describing the final velocity as a fraction, $f < 1$, of the initial velocity, the result is:

$$\Delta KE = \frac{mv_i^2}{2}\left(f^2 - 1\right). \tag{2.2.3}$$

Note that ΔKE will always be negative – kinetic energy of the bicycle and rider is always lost during braking operations.

Based upon ideas presented in the previous section, a simple model was developed to estimate the kinetic energy which could be captured during typical braking operations and used to power LED safety flashers. The model assumes that cyclists must minimally use brakes when approaching red lights at major intersections. According to Prof. Peter Furth [8], since signals at major intersections in cities are not coordinated for bicycle traffic it is appropriate to assume that a cyclist will arrive at any given traffic signal at a random point in its (green-yellow-red) cycle. The duration of the red light is typically ~ 35 seconds, so for a typical 70 second, two-stage traffic signal, the probability that a traffic signal will be red, P_{red}, on approach is simply the ratio of the "red time," t_{red}, to the total period of the traffic signal, T_{sig}:

$$P_{red} = {t_{red}}/{T_{sig}} \,. \tag{2.2.4}$$

If the total number of traffic signals, N_{sig}, for a single trip is known, the total energy available for capture during braking may be estimated as:

$$E_{tot} = N_{sig} P_{red} \frac{m v_i^2}{2} \left(1 - f^2\right). \tag{2.2.5}$$

Dividing both sides of Eq. 2.2.5 by the total trip time, T_{tot}, gives a relationship that describes the average power, P_{avg}, available continuously during the trip:

$$\frac{E_{tot}}{T_{tot}} = P_{avg} = \frac{N_{sig} P_{red}}{T_{tot}} \frac{m v_i^2}{2} \left(1 - f^2\right). \tag{2.2.6}$$

Though Eq. 2.2.6 may be solved for a known travel route, it is still not very descriptive of urban cycling in general. Fortunately, since traffic signal spacing is known to be consistent, the N_{sig}/T_{tot} term is simply another way of representing the cruising velocity, v_i. Where f_{sig} is the number of traffic signals per unit distance in urban areas,

$$\frac{N_{sig}}{T_{tot}} = f_{sig} v_i \,. \tag{2.2.7}$$

Therefore, from Eq. 2.2.6, an estimate of the average continuous power available to LED flashers from regenerative braking during city riding is:

$$P_{avg} = f_{sig} P_{red} \frac{m v_i^3}{2} \left(1 - f^2\right). \tag{2.2.8}$$

Traffic signals in cities such as Boston or Chicago are generally placed at quarter-mile intervals; in suburban areas, half- or one-mile signal spacing is more common [9, 10]. For this model, it is assumed that for typical commuter cyclists, $f_{sig} = 2 \text{ mi}^{-1} \approx 1.2\times10^{-3} \text{ m}^{-1}$. Taking $f =$ 0.75 indicates that one fourth of the total decrease in velocity is due solely to regenerative braking. Thus, for typical values of $v_i = 15$ mph ≈ 6.7 m/s and $m = 100$ kg, the average continuous power available to LED flashers is:

$$P_{avg} = \left(1.2\times10^{-3}\text{m}^{-1}\right)\left(\frac{35\text{ s}}{70\text{ s}}\right)\frac{(100\text{ kg})(6.7\text{ m/s})^3}{2}\left(1-(0.75)^2\right) \approx 4\text{ W} \,. \tag{2.2.9}$$

This estimate indicates that there is about one order of magnitude more energy available than is needed to power typical 0.6 W LED rear safety flashers. It also suggests that with appropriately

high efficiencies for energy conversion and storage, powering 2.4 W high-power LED headlamps may also be feasible.

2.3. Motor sizing and selection

The conversion of kinetic mechanical energy to stored electrical energy requires a suitable motor or generator. Ideally, the motor would be sized to capture all or most of the kinetic energy for storage during a braking operation, such that dissipative friction brakes would not be necessary. However, this is simply not possible on bicycles, where size and weight are major constraints. For the worst-case scenario of maximum deceleration (~ $0.5g$, as from Sec. 2.1) at high velocity (~ 30 mph), the peak power, P_{peak}, dissipated when the brakes are first engaged is:

$$P_{peak} = mav_i \approx 7000 \text{ W} . \tag{2.3.1}$$

Generators capable of capturing all of this energy would be too large to mount on bicycle brake calipers. For comparison, 7 kW generators are sold as standby power supplies to meet the energy needs of small homes during power outages [11]! Since the power required for "hard braking" is beyond the capabilities of small DC motors, dissipative friction brakes must be used in combination with a regenerative system for the safety of the cyclist. Further, it should be noted that even feathered braking operations will not produce useful decelerations unless the motor is of sufficient power.

Table 2.3.1 below includes predictions of the rotational speed of the motor for a variety of gear ratios and extreme cycling velocities. As will be discussed further in Sec. 2.4, the need for a step-down voltage regulator or battery requires the selection of a higher voltage DC motor, which will achieve or exceed ~ 5 V even at low cycling speeds. Thus, it is important to select a motor and gear ratio combination from the table below where the maximum allowable rotor speed (also max. voltage) is roughly that for a bicycle velocity of 30 mph (~ 50 km/h).

Table 2.3.1: Tabulated values for rotor speed as a function of:
1) the ratio of the motor wheel diameter, d, and the diameter, D, of the tire rim, and
2) the velocity of the bicycle.

	Rotational speed of rotor [rpm]			
Rotor/tire gear ratio, d/D =	0.022	0.043	0.087	0.130
$\omega_{typ}(v_i = 15 \text{ mph}) = 652$ rpm	29.8 k	14.9 k	7.46 k	4.97 k
$\omega_{typ\,max}(v_i = 30 \text{ mph}) = 1304$ rpm	597 k	29.8 k	14.9 k	9.94 k
$\omega_{typ\,low}(v_i = 1 \text{ mph}) = 43$ rpm	1.97 k	984	492	328

For a 90 W motor with a maximum allowable rotor speed of ~ 9 krpm, Table 2.3.1 indicates that a gear ratio of 0.13 would be appropriate. Since the rim for typical 26 in. mountain bike tires are located at a diameter of ~ 23 in., the diameter of the motor contact wheel would be 0.13 × 23 in. ≈ 3 in. In the prototype discussed in this work, a smaller (d = 1.75 in.) motor contact wheel is

used to obtain greater power regeneration capacity at lower cycling speeds since mountain bike used will not reach speeds of 30 mph.

In summary, proper motor selection will determine the effectiveness of the final system. Given the tight space constraints of bicycle brake calipers, it becomes important to choose a motor with the highest rated power so that braking operations will provide useful deceleration for the cyclist. For both voltage regulation and battery charging, it will additionally be critical to select a motor capable of exceeding the minimum "lockout" voltage and the charge threshold voltage, respectively. DC brush motors with rare earth magnets are widely available, which fulfill all of the above requirements; they are ideal for this type of application.

Though slightly larger than desired, a 90 W Maxon RE 35 motor at 48 VDC was selected for reasons of availability. One benefit of choosing such a motor, however, is the complete lack of "cogging" effects common in cheap high-power DC brush motors, which tend to resist rotation of the motor shaft. This could cause the motor contact wheel to slip on the rim of the tire.

2.4. Energy storage

To store the energy captured by the motor/generator during braking, the system must include a bank of batteries or supercapacitors. In this work, because the primary focus is on the mechanical design and a proof of concept, AA NiCd batteries were selected. Though supercapacitors can accept energy at much higher rates when compared with batteries, any over-voltage would damage the supercapacitors. Rechargeable NiCd batteries are sufficient for the storage needs of this work, cost less, and are less delicate.

In the prototype system, the motor terminals are connected in parallel with the battery bank and voltage regulator input terminals. As shown in Fig. 2.4.1 below, a full-wave bridge is placed between the motor and the rest of the system, so that current does not flow from the batteries to power the motor and so that the motor may rotate in either direction to generate a positive voltage across the battery terminals.

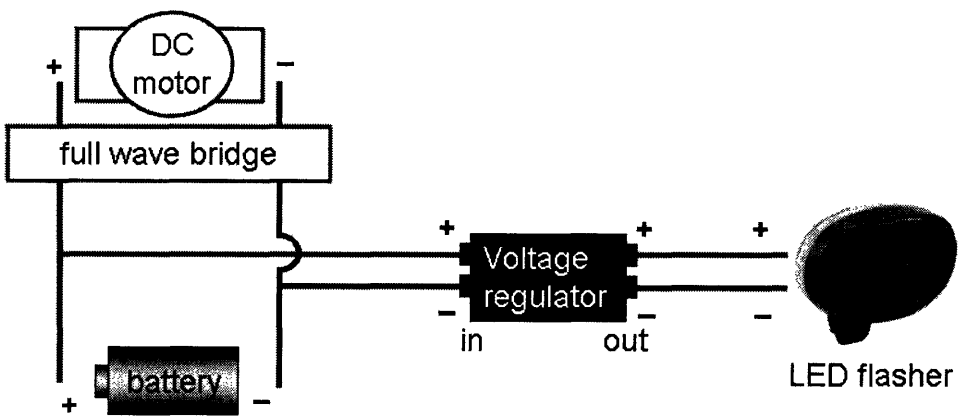

Figure 2.4.1: Schematic of energy storage and LED flasher circuit. The full wave bridge prevents current from flowing from the battery in the direction of the motor.

One limitation that arises from this setup is that no current will flow from the motor through the bridge if the voltage across the motor terminals is lower than the voltage of the battery bank. Since the Maxon RE 35 motor used in this work has a speed constant of 80.6 rpm/V and the voltage across the NiCd battery bank is roughly 5.2 V, the motor will not charge the batteries for bicycle less than 0.73 mph.

The system must also include a way of converting the dynamically changing input voltage from the motor and batteries to supply a constant, low voltage to the LED safety flashers. For this purpose, a LM2575 adjustable step-down switching voltage regulator is used. The circuit diagram used is shown below in Fig. 2.4.2. The feedback resistors R_1 and R_2 were selected to provide the LED flashers with a constant V_{out} = 3 V.

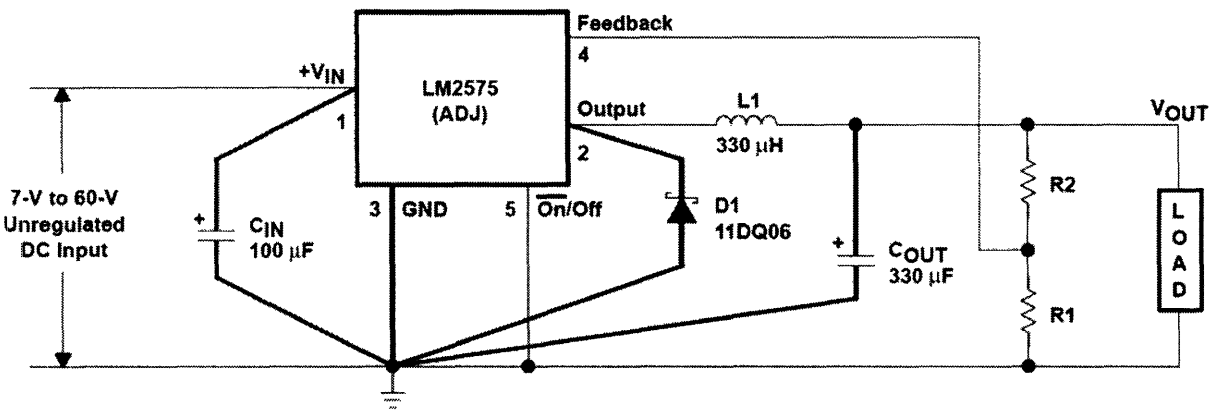

Figure 2.4.2: Circuit diagram for LM2575 step-down switching voltage regulator used to protect the LED safety flashers from spikes in voltage from the motor/generator. R_1 and R_2 were selected such that the output, V_{out} = 3 V [12].

3. Brake Caliper Design

3.1. Design with a user focus

When choosing a design for a prototype regenerative braking system, it is necessary to understand the needs and habits of those commuter cyclists who might use such a system. The first point to consider is that brake calipers are not consistent across different types of bicycles. Road bikes, for example, use different mounting hardware and mechanisms for braking than do mountain bicycles. Since the regenerative braking system described by this work would be most effective in urban areas where braking is more frequent, the urban commuter cyclist is of primary importance.

The mountain bicycle is commonly used for city commutes due to its rugged design. The fatter, treaded tires are less responsive than those of road bikes, but are better for jumping curbs or riding over potholes and through gravel. Except those with disc brakes installed, mountain bikes also have common brake mounting points at the backstays and front fork. These can accommodate both cantilever brakes and direct-pull or V-Brakes. For the reasons above and because of availability, the prototype braking system in this work was designed to fit the mounting points of standard mountain bikes.

The direct-pull geometry of Fig. 2.1.1 was chosen as a basis for the design of the calipers and friction pads, primarily because of their high mechanical advantage when compared to cantilever brakes. Also, for a motor as large as the Maxon RE 35 used in this work, the reduced angular rotation about the mounting point on the fork decreases the chance that the rear of the motor could impact the spokes of the wheel as the brake is released.

The emphasis on utilizing familiar brake geometry is intended to assist the potential users in understanding the function and utility of a regenerative braking system, which provides improved safety (LED flasher) at no additional cost. Without the *integration* of a regenerative system with familiar friction brakes, the system could easily be confused at first glance with one of the common wheel contact generators associated with increased physical effort and "generator drag." This distinction is even more difficult to convey in the case of hub-integrated generators, which has a lower profile and no visible mechanical contact with the moving wheel. Ignoring the drawbacks of eddy currents altogether, cyclists who do not understand the basic principles of thermodynamics may not even consider the notion that the energy used to power lights and flashers results directly from increased physical effort on their part. One bicycle store clerk refused to believe that hub-integrated generators contributed any drag whatsoever since the rotor does not physically come into mechanical contact with the windings.

3.2. Iterative brake caliper design using CAD

Computer-aided drafting (CAD) techniques enabled the rapid visualization of multiple design concepts, which provided the insight necessary for finalizing the prototype design. Manipulation of virtual components in the CAD environment elucidated the need for a completely new brake caliper as well as the importance of maintaining several degrees of freedom for an adjustable motor contact wheel.

Partly to improve the end user's understanding of how the system works, and partly to save time, the design of the mechanical components of the system began with an effort to utilize points of attachment on existing, familiar bicycle brake calipers. Shown below in Fig. 3.2.1 is a concept, which attaches to the brake caliper at the friction pad mount.

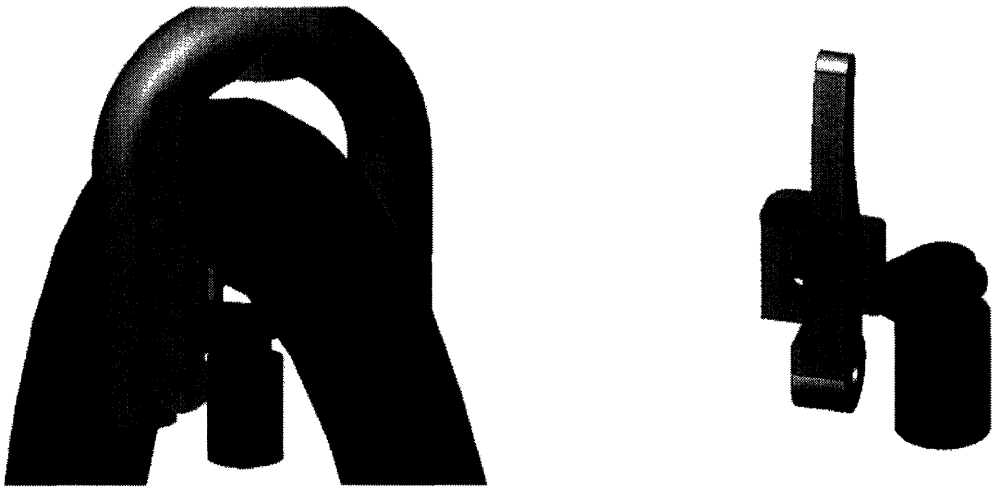

Figure 3.2.1: Design concept for attaching a motor for regenerative braking to an existing brake caliper.

In this design as the brake caliper is engaged, the motor contact wheel touches the rim first. As additional force is supplied at the brake handle, the motor remains in contact with the rim, but allows a friction pad to bear against the rim through rotation about a pivot. The main problem with this concept is that there are too few degrees of adjustability. It is clear even from the drawing above that the motor contact wheel would not be tangent to the rim.

In a subsequent CAD exploration, a concept, which required the design of an entirely new brake calipers was generated. As shown in Fig. 3.2.2, the concept includes a linear motion of the motor contact wheel. In the figure, a spring would be placed between the caliper itself and the motor contact wheel.

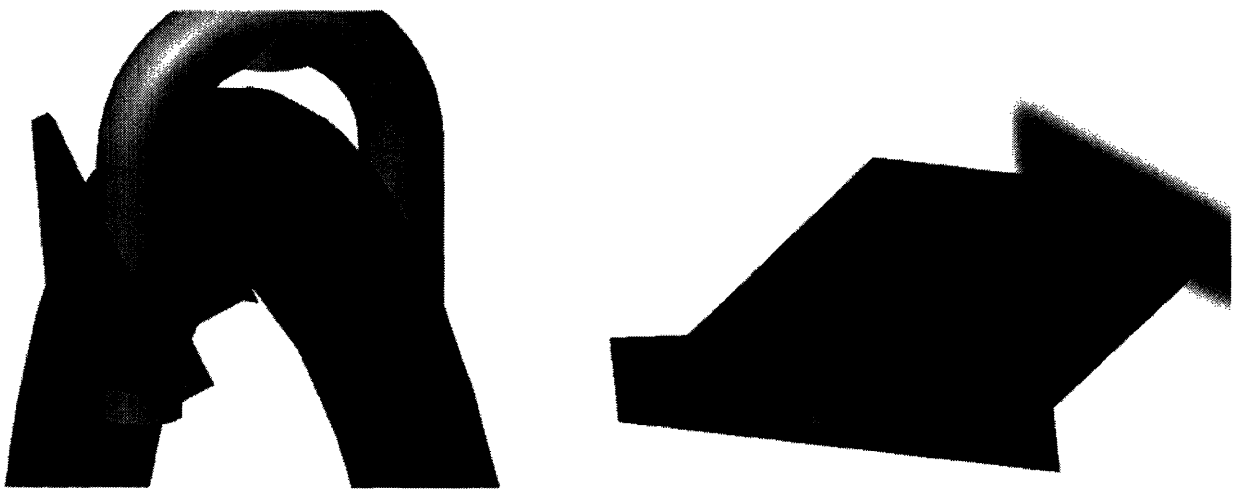

Figure 3.2.2: A concept for a new brake caliper in which the motor contact wheel is placed at the center of the friction pad.

The main advantage of this design is that the braking force follows a linear path through the wheel contact point, axis of rotation, and the center of the friction pad. No torque is introduced, which would tend to twist the brake calipers in undesired ways. A key problem with the design, however is that it would likely jam if the slot at the center were exposed to dirt or the elements. As most bicycles are used outdoors, this design would most likely become problematic for users after a year or so.

Taking lessons from both of the above CAD explorations, a final prototype design was chosen, which required the design of an entirely new brake caliper. Shown below in Fig. 3.2.3, the brake calipers are designed to use the same restoring springs and method for attaching to the fork and backstays of mountain bikes as the direct-pull brake of Fig. 2.1.1.

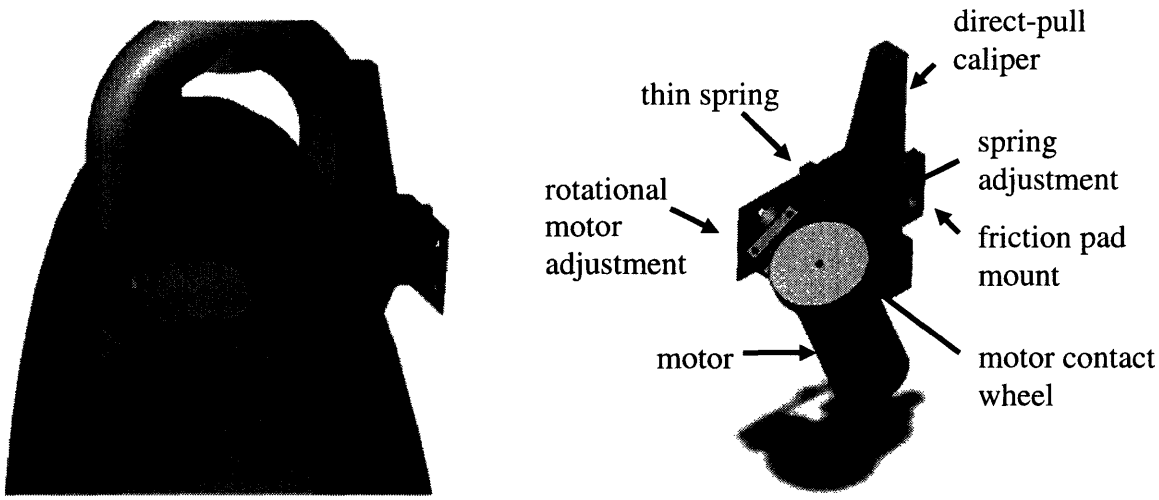

Figure 3.2.3: A CAD illustration of the final concept developed as a prototype regenerative brake caliper in this work.

As force is applied to the brake handle, the brake calipers both rotate toward the wheel of the bicycle. The motor contact wheel touches the rim first, followed by a friction pad, should additional braking force be applied by the rider. A thin spring is used to couple the motor with the brake caliper, such that the brake calipers may continue to rotate toward the wheel even as the motor wheel is in contact with the rim. Additionally, the angle and position of the motor contact wheel is adjustable in 3 dimensions, ensuring correct tangency to the rim of the bicycle tire.

3.3. Manufacture of custom direct-pull brake calipers

The following Figs. 3.3.1-3.3.2b are photographs of the final prototype regenerative brake calipers. These were manufactured primarily from aluminum and brass according to the dimensions in the CAD drawings of Fig. 3.2.3. Visible in Fig. 3.3.1, the restoring springs were

formed from spheroidized air-hardening steel using v-brake restoring springs as a template. They were then hardened and tempered using a furnace to increase their springback and the bulk stiffness of the brake calipers. As noted below, an adjustment screw was placed to locate the motor contact wheel in the direction perpendicular to the bicycle tire plane.

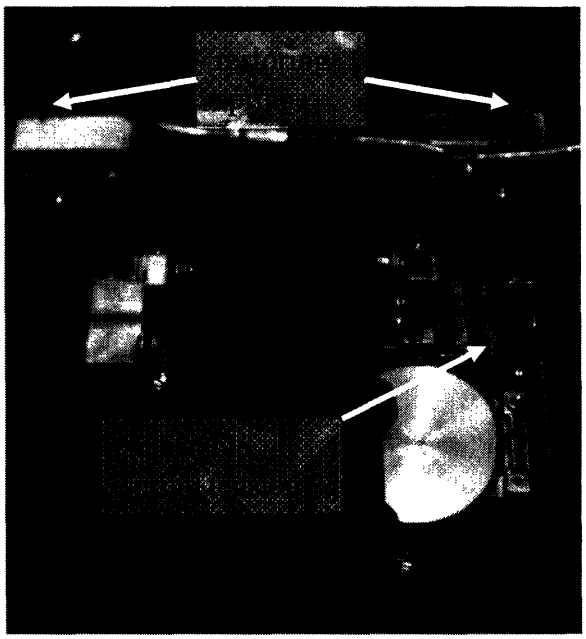

Figure 3.3.1: View of brake calipers and motor/generator wheel from above.

Shown as dark gray in Fig. 3.2.3, but absent from the caliper at the left in Fig. 3.3.1 above, is a free-spinning wheel, which was designed to balance the force of the motor contact wheel. In practice, it was found to be unnecessary due to the much higher stiffness of the tempered restoring springs.

Figs. 3.3.2a and 3.3.2b highlight some additional features and details of the prototype, which are absent or different from the solid model of Fig. 3.2.3. Most notably, the profile of the calipers was changed significantly from that of the CAD model to permit clearance of the tire treads. Also important is the rubber o-ring for frictional contact with the aluminum rim of the bicycle wheel. A groove was cut on the circumference of the motor wheel to tightly fit a standard o-ring allowing for replacement in case of damage or wear.

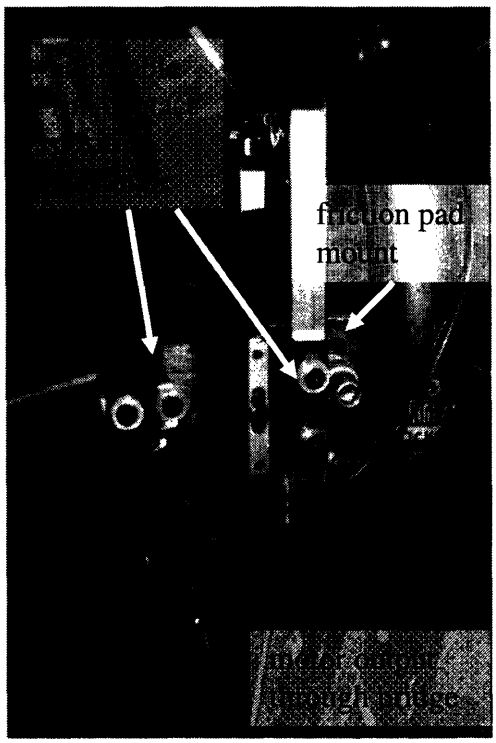

Figure 3.3.2a: View of brake calipers and front fork of bicycle from the side.

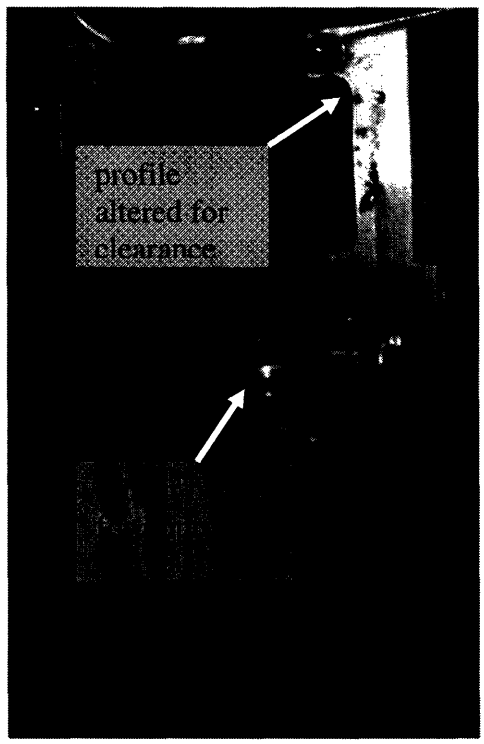

Figure 3.3.2b: View of brake calipers and front fork of bicycle from the front.

The cantilevered spring coupling the motor with the brake caliper was cut on a water-jet cutting machine from 0.020 in. thick tempered steel sheet. The spring was designed to be very stiff in the direction of the fork to support the weight of the motor and somewhat compliant in the perpendicular direction – allowing for rotation about the primary axis of the brake caliper.

4. Testing

4.1. Measuring voltage and current flow during braking operations

Shown below in Fig. 4.1.1 is a schematic of the prototype regenerative braking system complete with instrumentation for measuring voltage and current.

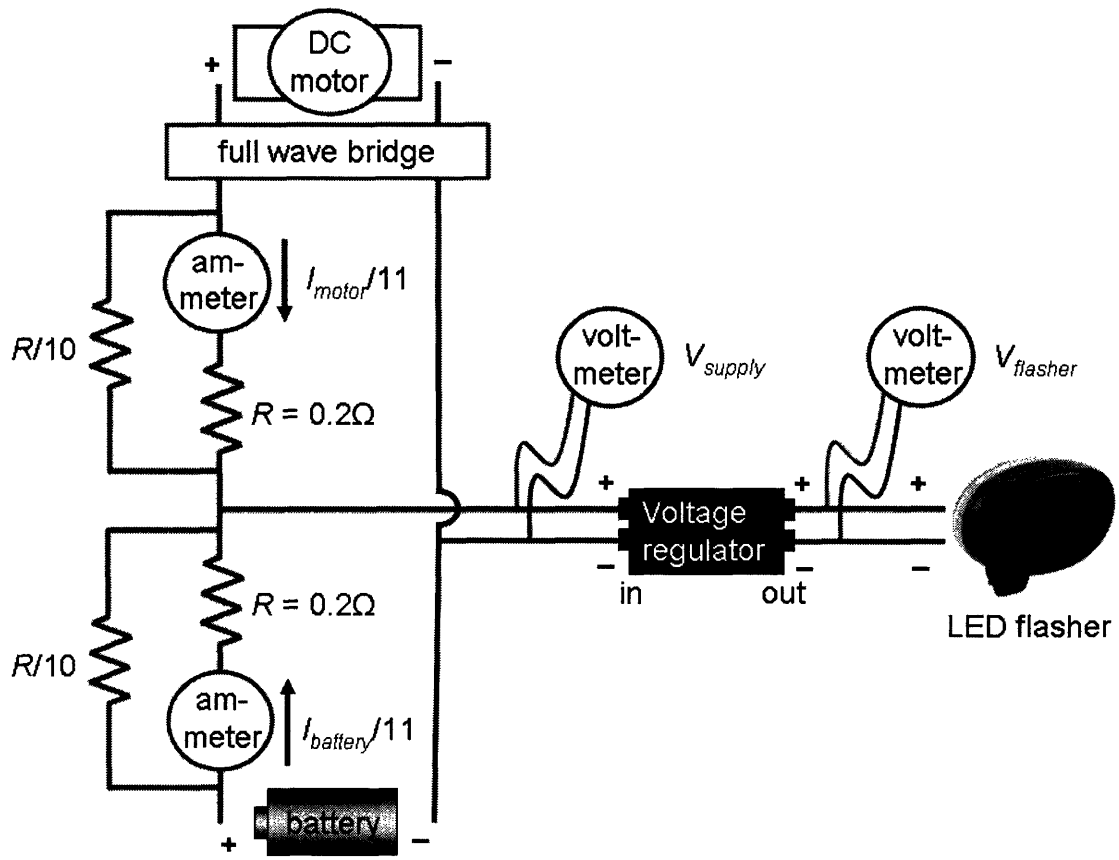

Figure 4.1.1: Schematic of setup used for testing the regenerative braking system. Resistors were put in parallel with the ammeters to maintain current levels below their rated value of 600 mA.

Since it was necessary to bring the bicycle up to normal cycling speeds during system tests, a remote method for data collection was necessary. Measurements of current and voltage from the ammeters and voltmeters shown in Fig. 4.1.1 were recorded using a battery powered Vernier LabPro® [13]. The use of the LabPro device restricted the types of voltage and current probes, which could be used. For example, the standard voltage and current probes were only rated for +/- 10 VDC and 600 mA, respectively. For the purpose of measuring higher currents, power resistors were placed in parallel with the current probes as shown in the diagram above.

Prior to brake caliper testing, the voltage regulator and LED flasher circuit were connected to the terminals of a lead-acid battery bank (different from the NiCd battery pack used otherwise) to

obtain an idea of what the system . The power out of the battery is shown below in Fig. 4.1.2 for both the pulse-width modulated (PWM) flashing mode and the continuous operation mode.

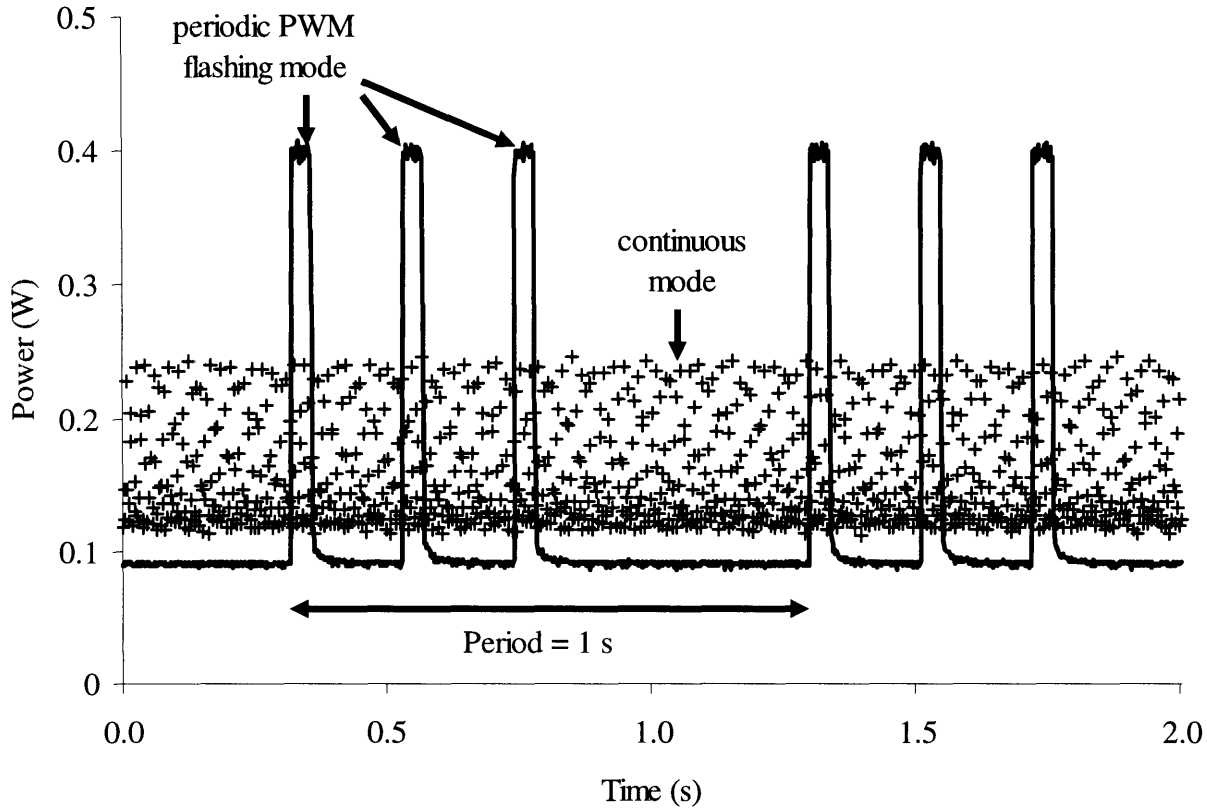

Figure 4.1.2: Power out of a 4 V lead-acid battery during continuous and PWM flashing mode LED flasher operation. The peaks in power during the PWM mode are due to a switching "on" of the LEDs. It is important also to note that the power does not go to zero between the peaks. Some of the remaining ~ 0.1 W powers the voltage regulator circuit.

During the testing of the prototype system, a Sigma Sport BC 500 Cycle Computer [14] positioned at the handle bar was used to visually monitor cycling speed on a liquid crystal display. When the desired speed of each test was reached, the brakes were immediately applied. Two types of braking operations were performed along a straight course of travel at speeds ranging from 8 mph to 19 mph:

1) motor wheel contact only, and
2) a full stop at ~0.2g deceleration.

Fig. 4.1.3 below shows data gathered for such a test at 15 mph. Note that during ~ $1 < t < 3$ s only the motor wheel is in contact with the rim of the wheel and that the subsequent full stop operation begins at $t = 4.5$ s.

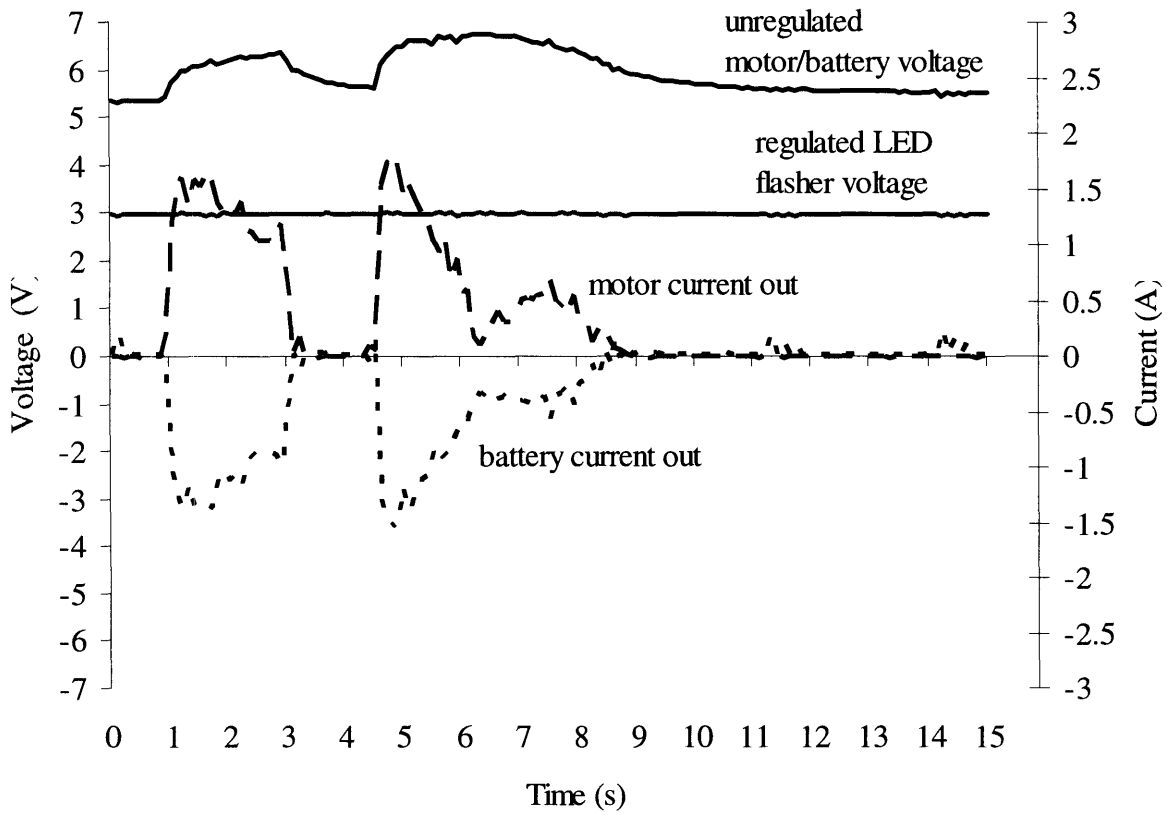

Figure 4.1.3: Plot of voltage and current as functions of time for several critical points during two consecutive braking operations at 15 mph. A current flowing from the positive terminal of the motor (long dashed line) indicates braking. For 1 s < *t* < 3 s, only the motor wheel was active and for 4.5 s < t < 10 s both the friction pad and the motor wheel were brought into contact with the rim or the tire.

The sharp drop in current from 3 to 0 A following the feathered braking operation is due to the release of the brake handle. A short release of the brake handle helped to distinguish separate braking operations and to show that the restoring springs of the brake caliper were working effectively to allow rim contact *only* during braking operations.

Since testing was performed indoors on a 1/8-mile track, it became impossible at speeds > 15 mph to feather the brakes, release the brake handle, and then complete a full stop all while maintaining a straight course. As such, at high speeds only a full stop braking operation was performed.

4.2. System efficiency and power analysis

The data from Fig. 4.1.3 were used to determine the flow of energy in the prototype system from the motor to the batteries and from the batteries to the voltage regulator and LED safety flasher. Using the familiar relationship for power $P = VI$ in an electrical circuit, the power flow

out of the battery and motor is shown below in Fig. 4.2.1. A negative power value for a battery indicates charging.

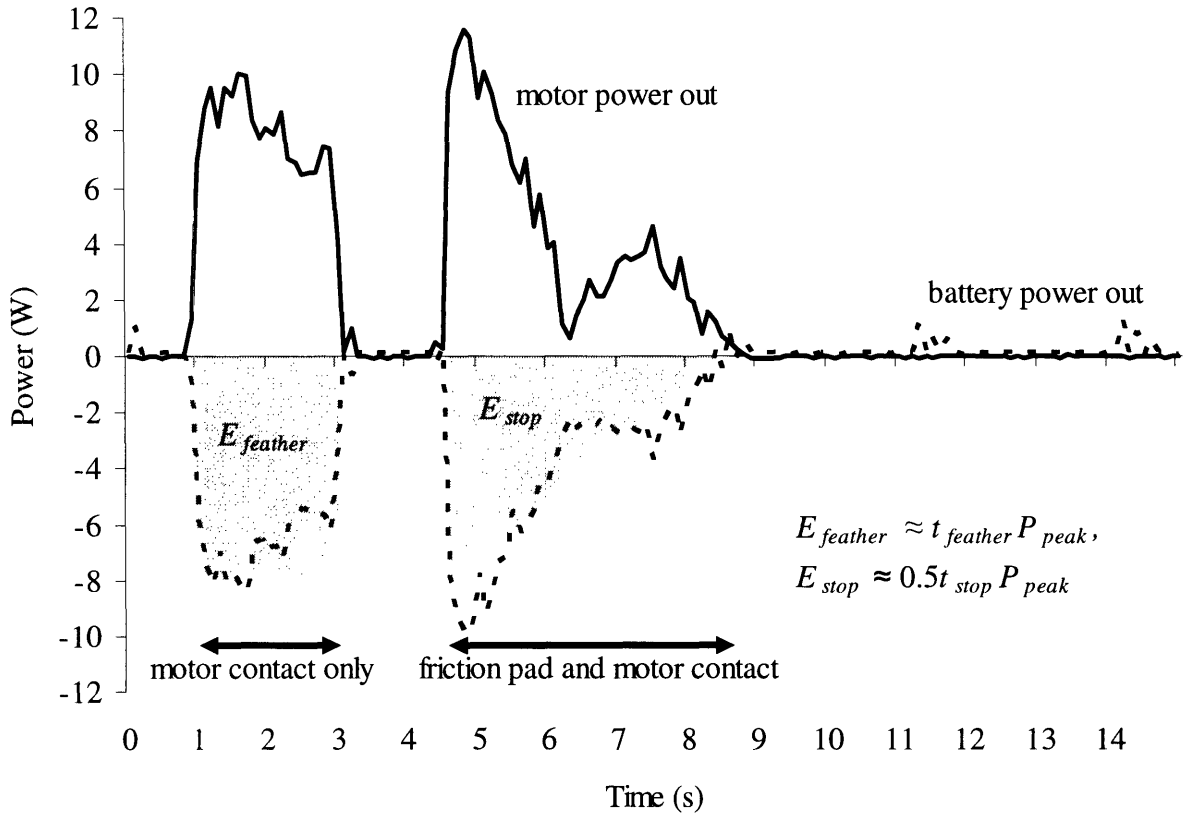

Figure 4.2.1: Plot of power generated by the motor and the flux of power into and out of the battery during feathered (motor contact only) and combined (friction pad and motor contact) braking at 15 mph. For the battery, a positive value for power indicates a flow of energy from the battery to the voltage regulator and LED flasher.

The efficiency of this conversion of power is obtained by dividing the power *in* to the battery bank by the power *out* of the motor. The efficiency of power conversion in Fig. 4.2.1 at a cycling speed of 15 mph was found to be nearly 79%.

It is important to note that during the feathered braking operation, the power out of the motor (into the battery) does not decrease noticeably. This suggests that during the $0.2g$ braking operation, most of the deceleration of the bicycle and rider is the result of dissipative braking. Thus, during a feathering operation, the total energy captured and stored is simply the product of the mean power into the batteries and the total time over which the brakes are applied.

In Fig. 4.2.2 the flux of power into the batteries is shown for initial cycling speeds ranging from 8 to 19 mph. As the speed of the bicycle increases, so does the energy stored.

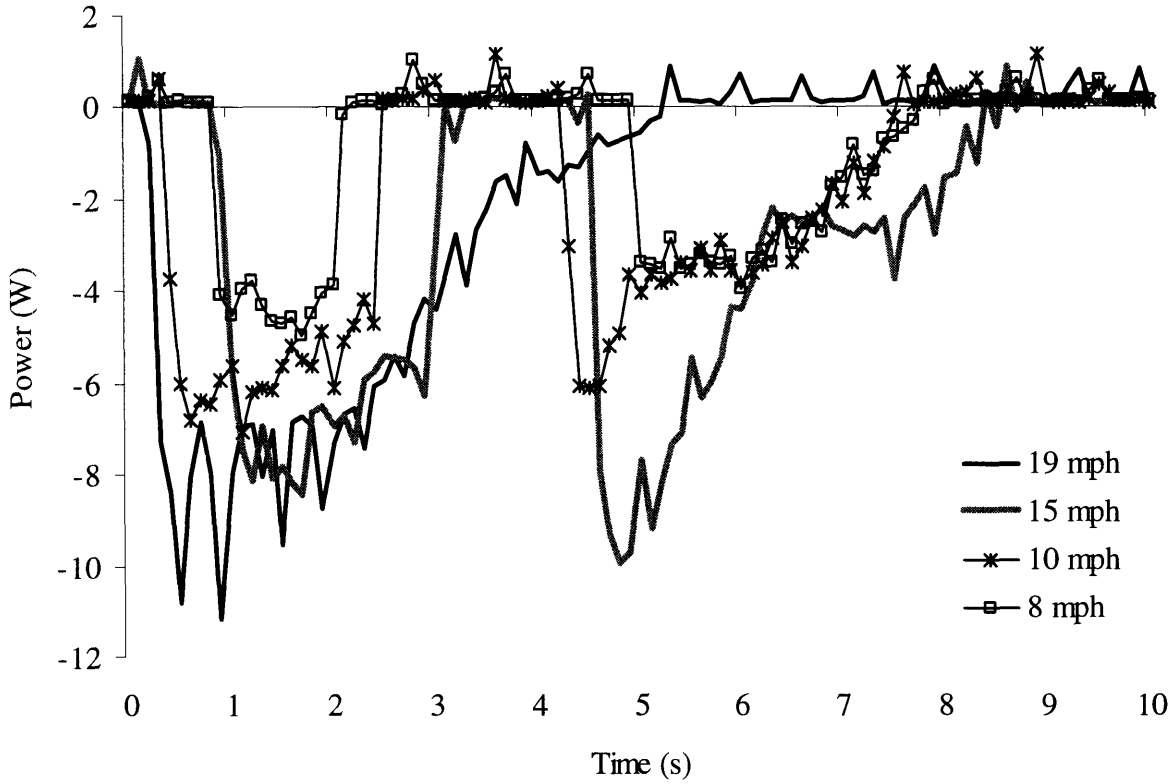

Figure 4.2.2 Power flow out of the battery during braking operations for several initial cycling speeds. Negative power values indicate battery charging.

If is assumed that urban commuter cyclists travel at a nearly constant speed and stop with some frequency over their total travel distance, the mean power available, $P_{available}$, during a commute may be calculated. In Table 4.1.1, this estimate is obtained for several stopping frequencies and cycling speeds. In each instance, it is assumed that the cyclist comes to a full and complete stop. The captured energy associated for each stop is $0.5 t_{stop} P_{peak}$, as in Fig. 4.1.2.

Table 4.1.1: The dependence of the ratio of power in ($P_{available}$ from braking) to power out (to LED flashers, P_{flash} = 0.18 W) on stopping frequency. Dark gray shading indicates cases where the system is capable of powering the LED flasher continuously. Light gray shading indicates cases where the system is capable of powering the system > 50% of the time.

Cycling speed [mph]	Energy stored per braking operation [J]		$P_{available}/P_{flash}$ dependence on travel distance per full stop		
	1 s feathering	full stop	1/8 mi.	1/4 mi.	1/2 mi.
8	4	5.5	0.54	0.27	0.14
10	6	10.5	1.0	0.52	0.26
15	8	14	1.4	0.69	0.35
19	8	20	2.0	0.99	0.49

The results tabulated above show that if the cyclist travels consistently at speeds greater than 10 mph, LED safety flashers drawing 0.18 W from the motor and batteries can be powered:

1) *continuously* for stopping frequencies of at least 8 per mile, and
2) *semi-continuously* for stopping frequencies of at least 4 per mile.

In other words, the commuter cyclist who travels only in low-light conditions would have to apply brake pressure about 8 times per mile, while a commuter who travels in low-light only 50% of the time would have to apply brake pressure half as frequently. Thus, this system would work well for a commuter in a city with 1/4-mile traffic signal spacing. If the commuter only needed to turn on the LED flashers during a return trip in the evening, then the power needs of the flashers would be completely met by the brakes and the batteries would not need to be replaced or recharged outside of the system.

4.3. Evaluation of braking model

The model proposed initially suggests that some fraction (~1/4 in Sec. 2.2.2) of the total decrease in bicycle speed due to braking can be captured exclusively by a regenerative system. The presumption that feathered braking operations typical of dissipative braking systems could be replicated by regenerative systems was clearly wrong in the case of the prototype developed in this work. Instead, it is apparent from Fig. 4.2.2 that during light braking operations at nearly constant speeds, the total storable energy is approximately proportional to the total time spent feathering the brakes, since so little deceleration is due to the motor/generator, itself. Thus, instead of observing the predicted 4 W of power available for battery charging/storage, a mere 0.2 W is measured as the power into the batteries if the mean cycling speed and braking frequency are sufficiently high.

As a result, instead of assuming that the regenerative braking component is responsible for a percentage decrease in cycling speed, it is more appropriate to assume a constant deceleration over a time, t_{brake}, and find the energy available, E, from a function of the power in to the batteries, $P_{charge}(\omega)$, as a function of motor/generator speed, ω.

$$E = P_{in}(\omega)t\,. \tag{4.3.1}$$

Consider an example of a cyclist moving at 10 mph, if the brakes are applied 2 times per mile for about 3 seconds on average each time. From Eq. 4.3.1, the mean power used for battery charging, P_{in}, is:

$$P_{in} = \frac{E}{t} = (2\ \text{mi}^{-1})(8\ \text{W})(3\ \text{s})(10\ \text{mph})\left(\frac{1\ \text{h}}{360\ \text{s}}\right) \approx 1.3\ \text{W}. \tag{4.3.2}$$

This result is still an overestimate, but is slightly more accurate than the 4 W predicted previously for the same conditions.

5. Conclusions and discussion

The current prototype. A novel method for powering LED safety flashers using regenerative braking has been presented in this work. Custom direct-pull calipers were designed to accommodate traditional friction pads and a DC motor/generator for the recovery of kinetic energy. In this way, the additional functionality of safety flashers has been added at no cost to the cyclist. Throughout the course of normal cycling and braking, a battery bank powering the LED safety flashers is re-charged. This improves dramatically upon hub-integrated and wheel contact generators currently available, which drain up to 14% of the rider's total physical effort at typical cycling speeds.

While it has been shown that the total kinetic energy dissipated during normal braking operations is very large compared with the energy needed to power LED safety flashers, not all of it can be captured with small DC motors. Even the rather large 90 W motor used in this work does not contribute nearly enough deceleration to feel like dissipative friction braking. Such a large motor or generator would be needed to feel such an effect that it would be impractical to mount on a bicycle. As such, it makes more sense to minimize the profile of the regenerative brake and use the smallest motors with the greatest power density. DC brush motors with rare earth magnets rated for 30-40 W would be ideal. At cycling speeds up to 19 mph, only 14% of the capacity was utilized for the 90 W motor in this work.

The simple step-down voltage conversion circuit used to protect the LED flasher from over-voltage worked well for a motor with a speed constant of 80.6 rpm/V and a gear ratio of 1:14. For energy storage, cost-effective NiCd batteries had sufficient power density and were able to store energy supplied by the motor at efficiencies near 79% on average.

The overall effectiveness of the regenerative braking system improves with increasing average cycling speed and with increasing stopping/braking frequency. For cyclists traveling at speeds greater than 10 mph, the LED safety flashers will operate *continuously* for a stopping frequency of 8 times per mile and *semi-continuously* (> 50% of the time) for a stopping frequency of 4 times per mile. These conclusions support the design and development of this system specifically for use by urban commuters. Since some commuters regularly travel in low-light conditions less than 50% of the time, even semi-continuous LED flasher operation may be suitable in areas where braking is not as frequent.

Ideas for future development. The most obvious next step for development of the system as it stands would be to guard it against sand, gravel, and weather. Though the mechanical components of the system were designed to work well, even when covered in grease or dirt, the motor, voltage regulator circuit, and battery pack would need to be packaged to prevent damage from water. An injection molded casing with appropriate rubber seals or gaskets would probably be sufficient. If a smaller, unsealed motor is used, additional protection would need to be considered to protect it against sand, grease, and water.

A second improvement, which would be needed for long battery life, is an appropriate charge controller. As is, the system does not guard against overcharging at all, which in the case of NiCd batteries could cause damage to the cells and hazardous venting [15]. Another solution

would be to instead use supercapacitors to store energy. Though somewhat expensive, they have an even higher power density than the NiCd battery used in the prototype and are capable of achieving efficiencies of nearly 90% - a ~ 10% improvement over the current efficiency. Fully charged, two 50 F supercapacitors at 2.5 V would have enough energy to power 0.2 W LED safety flashers for nearly 26 minutes. Improving the efficiency in this way would improve the function of the regenerative braking system in areas where stopping frequency is less frequent.

6. References

6.1. Cited references in order of appearance

[1] Juden, Chris. "Dynotest." *Cycle Touring and Campaigning*, Feb/Mar 1998. Cyclists Touring Club. Surrey, Great Britain. <http://www.myra-simon.com/bike/dynotest.html>

[2] "Injuries to Bicyclists" From a monograph by the Johns Hopkins Injury Prevention Center Sponsored by the Snell Memorial Foundation. <http://www.smf.org/articles/injury.html>

[3] "Bicycle Crash Statistics." Massachusetts Bicycle Coalition. 2002. <http://www.massbike.org/info1/stats.htm>

[4] Cat Eye Home Page. Cat Eye Co. Inc. 2004. <http://www.cateye.com/en/index.php>

[5] Luxeon Product Home Page. Lumileds Lighting, L.L.C. 2005. <http://www.luxeon.com/products/>

[6] Wilson, David Gordon. Bicycling Science. 3 ed. Chapter 7: Braking. pp. 237-261. Cambridge: MIT Press, 2004.

[7] Forester, John. Effective Cycling. 6 ed. pp. 205-208, 378-387. Cambridge: MIT Press, 2001.

[8] Furth, Peter. Chair, Department of Civil & Environmental Engineering, Northeastern University. 15 Feb., 2005.

[9] "Access Management." Issue Brief 13. U.S. Department of Transportation Federal Highway Administration and the Institute of Transportation Engineers. Apr., 2004. <www.ite.org/library/IntersectionSafety/access.pdf>

[10] Levinson, Herbert S. "Street Spacing and Scale." Urban Street Symposium Conference Proceedings. Dallas, TX. Jun. 28-30, 1999. <http://www.mackblackwell.org/research/finals/arc9012/streetspacing.pdf>

[11] 7,000 Watt Automatic Home Standby Generator System. Briggs & Stratton Product Catalog. Briggs & Stratton Power Products. 2004. <http://www.standbygeneratorsystems.com/products/7kw.cfm>

[12] "1-A Simple Step-Down Switching Voltage Regulator." Texas Instruments. April 2005. <http://focus.ti.com/lit/ds/symlink/lm2575-33.pdf>

[13] Vernier LabPro User's Guide.Vernier Software & Technology. 2000.

[14] Sigma Sport US Home Page. Sigma Sport Germany. 2005. <http://www.sigmasport.com/index_usa.html>

[15] "Nickel Cadmium Application Manual." Moltech Power Systems, Inc. 2000. <http://www.moltechpower.com/techdata/appmanuals/NiCd_Application_Manual.htm>

6.2. Additional references in alphabetical order

"A Compendium of Statistics from Various Sources." Bicycle Helmet Safety Institute. 25 Mar., 2005. <http://www.bhsi.org/stats.htm>

Ballantine, Richard. Richard's 21st-Century Bicycle Book. pp. 33-34. New York: Overlook Press, 2001.

"Bicycle Lighting." Wikipedia. 31 Mar., 2005. <http://en.wikipedia.org/wiki/Bicycle_lighting>

Kifer, Ken. "How to Avoid Traffic Accidents." Ken Kifer's Bike Pages. 1999. <http://www.kenkifer.com/bikepages/traffic/accident.htm>

"Police Safety Tips and Information." City of Auburn, Indiana Home Page. 2004. <http://www.ci.auburn.in.us/departments/police/safety_tips/>